transition point, the effect on bubble interactions is to reduce the range of the attractive force from ~100 nm to 55 nm[13]. It seems that such salts act to prevent bubble coalescence by reducing the range of the attraction between bubbles. Any explanation for the combining rules that emerge from the table shown in Fig. 2 must then be directly related to the effect of electrolytes on the hydrophobic interaction. As such, this table may provide insight into the mechanism of the hydrophobic interaction.

Finally, it is interesting to note that the salt level in the human body, marked by an arrow in Fig. 1, corresponds to the concentration where the onset of maximum coalescence prevention was achieved in the bubble chamber experiments. This surprising result indicates a possible link between salt levels and susceptibility to decompression sickness, as small bubbles present in tissue do less damage than larger bubbles. □

Received 16 November 1992; accepted 15 June 1993.

1. Klasson, V. I. & Mokrousov, V. A. *An Introduction to the Theory of Flotation* (Butterworths, London, 1963).
2. Israelachvilli, J. N. & Pashley, R. M. *Nature* **300**, 341–342 (1982).
3. Pashley, R. M., McGuiggan, P. M., Ninham, B. W. & Fennell Evans, D. *Science* **299**, 1088–1089 (1985).
4. Claesson, P. M., Blom, C. E., Herder, P. C. & Ninham, B. W. *J. Coll. Int. Sci.* **114**, 234–242 (1986).
5. Rabinovich, Y. I. & Derjaguin, B. V. *Coll. Surf.* **30**, 243–251 (1988).
6. Christenson, H. K., Claesson, P. M. & Pashley, R. M. *Proc. Ind. Acad. Sci. (Chem. Sci.)* **98**, 379–389 (1987).
7. Christenson, H. K. & Claesson, P. M. *Science* **239**, 390–392 (1988).
8. Christenson, H. K., Fang, J., Ninham, B. W. & Parker, J. L. *J. phys. Chem.* **94**, 8004–8006 (1990).
9. Lessard, R. R. & Zieminski, S. A. *Ind. Eng. Chem. Fundam.* **10**, 260–269 (1971).
10. Collins, G. L. & Jameson, G. J. *Chem. Eng. Sci.* **31**, 985–991 (1976).
11. Chan, D. Y. C. & Horn, R. G. *J. chem. Phys.* **83**, 5311–5324 (1985).
12. Blake, T. D. & Kitchener, J. A. *J. chem. Soc. Farad. Trans. I.* **68**, 1435–1442 (1972).
13. Cain, F. W. & Lee, J. C. *J. Coll. Int. Sci.* **106**, 70–85 (1985).

Reconstructing sea surface temperature and salinity using $\delta^{18}O$ and alkenone records

Frauke Rostek*§, Götz Ruhland†, Franck C. Bassinot*, Peter J. Müller†, Laurent D. Labeyrie‡, Yves Lancelot* & Edouard Bard§

* Laboratoire de Géologie du Quaternaire, CNRS, Marseille, France
§ Laboratoire de Géoscience de l'Environnement, JE DRED 192, Université d'Aix-Marseille III, France
† FB Geowissenschaften, Universität Bremen, FRG
‡ Centre des Faibles Radioactivités, CNRS-CEA, Gif-sur-Yvette, France

THE oxygen isotope ($\delta^{18}O$) composition of foraminiferal tests from deep-sea sediments is widely used as a palaeoclimate proxy, but it includes contributions from sea surface temperature, global ice volume and local salinity, which are difficult to separate. Recently a new technique for deriving palaeotemperatures has been developed which is based on the abundance ratios of unsaturated alkenones in phytoplankton algae[1,2]. Here we use a combination of oxygen isotope and alkenone records in a deep-sea core from the juncture of the Arabian Sea and the Bay of Bengal to extract the salinity signal from the former record. Variations in salinity are related to the balance between evaporation and precipitation[3], and are thus a sensitive indicator of climate change. Our 170-kyr salinity record enables us to reconstruct changes in the Indian monsoon over this period, considerably extending earlier studies (which reached back to 18 kyr ago)[4–8]. Like these previous studies, we find that large variations in the monsoon occurred during the transition from the last glacial period to the present interglacial, but our results also provide a view of the monsoon throughout the last glacial and demonstrate the potential of this approach for reconstructing palaeosalinity.

Variations of sea surface salinity are strongly related to the evaporation–precipitation ($E-P$) balance[3] and thus represent a sensitive climate indicator. Due to extreme monsoonal atmospheric and oceanographic gradients[9,10] (Fig. 1), the Northern Indian Ocean is characterized by two main surface water masses: high-salinity surface water (35–36.5‰) due to strong evaporation in the Arabian Sea and low-salinity water (31–34‰) in the Bay of Bengal caused by high precipitation and large river runoff, particularly during the SW monsoon[11].

In order to reconstruct climate variability in the Equatorial Indian Ocean, Core MD900963 (05° 04′ N, 73° 53′ E; 2,450 m water depth; Fig. 1) was recovered on the eastern shoulder of the Maldives Islands (SEYMAMA expedition, 1990; RV *Marion Dufresne*). Situated between the Arabian Sea and the Bay of Bengal, Core MD900963 is probably ideally located to monitor the changes of the monsoon during the last glacial cycle. A detailed $\delta^{18}O$ stratigraphy was established on the surface dwelling planktonic foraminifer *Globigerinoides ruber* (*white*) for the 54-m long piston core (Fig. 2*b*). The timescale was obtained[12] by tuning the $\delta^{18}O$ record to the SPECMAP record[13].

We measured the alkenone unsaturation ratio $U^{K'}_{37}$ (refs 1, 2) on the uppermost 10 m of the core to determine sea surface temperature (SST) variations for the last 170,000 years using the temperature equation of Prahl *et al.*[14]. Alkenone measurements were carried out at intervals of 10 cm at the Department of Geoscience of the University of Bremen. Sample preparation and technical details are described elsewhere[15]. Preliminary observations of the coccoliths indicate that *Emiliania huxleyi* and other species of the family *Gephyrocapseae* are abundant in the first 10 m of Core MD900963 (L. Beaufort, personal communication).

SST variations during the last 170,000 years are rather small—between 25.5 and 28 °C (Fig. 2*a*). Low SST values of ~25.5–26.5 °C are observed in oxygen isotope stages 4 and 3 with a minimum centred within stage 3. Interglacial stage 5 is characterized by high SST's between 27 and 28 °C. For stage 6, the SST's are ~1.5 °C higher than those observed in the stage 3 minimum.

Our data agree with SST reconstructions based on foraminifera assemblages from the tropical Indian Ocean[16] and in particular with the record published by Clemens *et al.*[17] The fact that these two SST time series (both obtained in the tropical

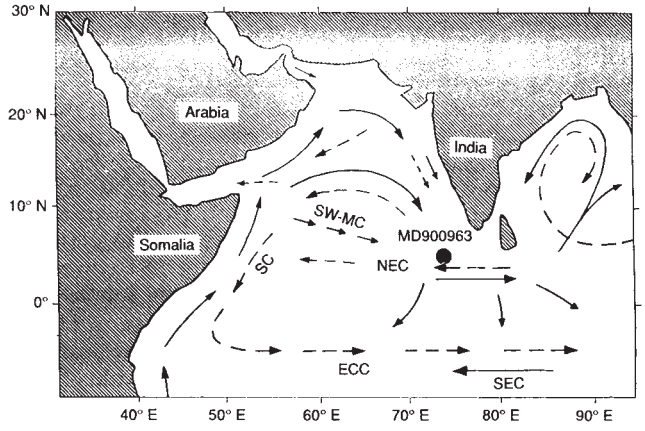

FIG. 1 Circulation patterns in the northern Indian Ocean[10] and location of Core MD900963. The solid lines represent the oceanic circulation during the SW monsoon (May to October), stippled lines the circulation during the NE monsoon (November to April). SC, Somali Current; NEC, North Equatorial Current; ECC, Equatorial Counter Current; SW-MC, SW Monsoon Current; SEC, South Equatorial Current.

Indian Ocean) are similar gives more confidence in the reliability of the U^K_{37} method. In particular, both records suggest that stage 6 was relatively warm and definitely not as cold as stage 3.

Changes in $\delta^{18}O$ recorded in planktonic foraminifera are controlled by global variations of seawater ($\delta^{18}O_{WG}$) due to the growth of continental ice sheets, and by local SST and $E-P$ changes. Sea surface salinity and local $\delta^{18}O_W$ of seawater are directly linked to the $E-P$ balance[18,19] and a linear correlation was found between these parameters for most of the global ocean[19]. The glacial to interglacial change in the oxygen isotope ratio for foraminifera ($\Delta\delta^{18}O_F$) can be expressed as follows[20]:

$$\Delta\delta^{18}O_F = a + b\Delta T + c(S - S^*) \quad (1)$$

where $\Delta\delta^{18}O_F$ is the measured deviation between modern and past $\delta^{18}O_F$ values of planktonic foraminifera, a represents global variations of sea water $\delta^{18}O_{WG}$ (variable through time due to changes of the global ice volume), b is the slope of the $\delta^{18}O_F$ versus temperature relationship, ΔT is the local temperature variation, c is the slope of the $\delta^{18}O_W$ versus salinity relationship, S is the past local salinity and S^* is the modern local salinity augmented with the global salinity change due to changes of the global ice volume. From equation (1), we obtained S by the following equation:

$$S = S^* + (\Delta\delta^{18}O_F - a - b\Delta T)/c \quad (2)$$

The salinity S^* varies through time in response to the sea level variations (for example 120 m of sea level lowering during the Last Glacial Maximum (LGM) compared with a mean ocean depth of about 3,800 m). Consequently S^* can be expressed as:

$$S^* = S_0^* + (SL \cdot 35/3800) \quad (3)$$

where S_0^* is the modern local salinity and 35‰ the modern mean ocean salinity, SL = sea level changes expressed in m below modern level (lowering being counted as positive).

Therefore, the past local salinity can be estimated by the following equation:

$$S = S_0^* + (SL \cdot 35/3800) + (\Delta\delta^{18}O_F - a - b\Delta T)/c \quad (4)$$

In order to provide an index of local salinity variations due to the local changes of the $E-P$ balance, we also calculated ΔS values expressed as:

$$\Delta S = S - S^* = (\Delta\delta^{18}O_F - a - b\Delta T)/c \quad (5)$$

The seasonal range of SST is very small (about 1–2 °C) at the location of core MD900963[11,21] and sediment trap studies[22–24] demonstrate that the *G. ruber* bloom does not lag significantly the abrupt increases in wind speed which corresponds to the beginning of the monsoons. Consequently, it is reasonable to use the U^K_{37} SST record to obtain ΔT, and to apply temperature correction to the $\delta^{18}O_F$ record ($b = -0.2$ for living *G. ruber* in the Indian Ocean[25]).

Labeyrie *et al.*[26] and Vogelsang[27] reconstructed a mean global seawater $\delta^{18}O_{WG}$ record for the past 200 kyr which is only affected by global ice volume changes. We normalized this seawater $\delta^{18}O_{WG}$ record to the global $\Delta\delta^{18}O$ value of 1.2‰, which has been established for the last deglaciation[28]. To estimate local salinity variations, changes in the global seawater $\delta^{18}O_{WG}$ (term a in equation (2)) have to be removed from the SST corrected $\delta^{18}O_F$ record of MD900963. Since a point-by-point subtraction of two independent isotopic records is very sensitive to phase differences and thus to timescale details, we first correlated the global seawater $\delta^{18}O_{WG}$ reconstruction to the timescale of the temperature corrected isotope record of Core MD900963 before subtracting it (Fig. 2*c*, we used the ANALYSERIE software developed by D. Paillard & L. D. Labeyrie, CFR Gif-sur-Yvette).

In order to reconstruct the $\delta^{18}O_W$ versus salinity relationship (term c in equation (2)), we used 52 seawater $\delta^{18}O_W$ and salinity measurements between 20° S and 21° N from the Arabian Sea (J. C. Duplessy, personal communication). Because no seawater $\delta^{18}O_W$ measurements are available for the Bay of Bengal, a

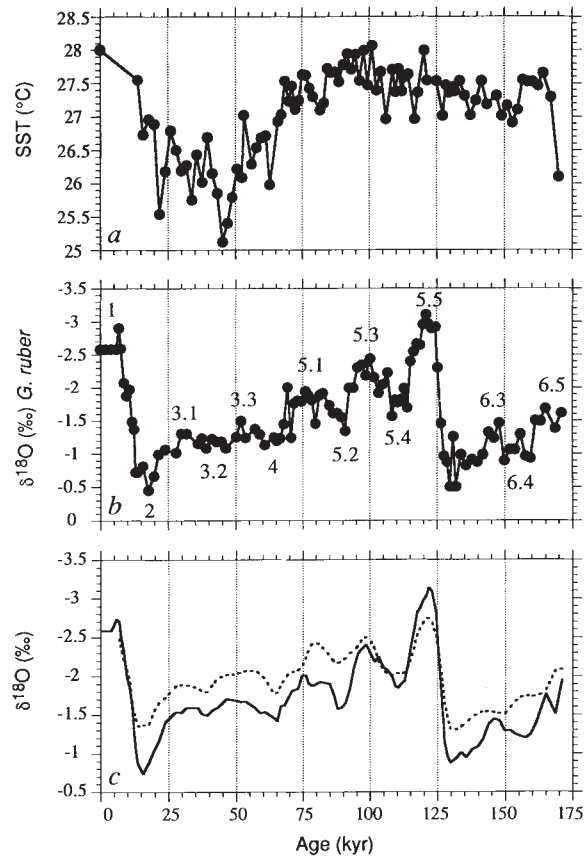

FIG. 2 SST (*a*) and $\delta^{18}O_F$ record (*b*) for Core MD900963. For missing core top SST and $\delta^{18}O$ values a constant modern annual mean SST of 28 °C (ref. 11) and a $\delta^{18}O$ value of −2.58‰ was used, assuming that sea level did not change during the last 6 kyr[28]. *c*, SST corrected $\delta^{18}O_F$ record (solid line) in comparison with the global seawater $\delta^{18}O_{WG}$ record[26,27] (broken line), correlated to the timescale of Core MD900963. Before calculation the raw data were smoothed using a least square procedure[31].

$\delta^{18}O_W$/salinity relationship was established by using 22 $\delta^{18}O_F$ *G. ruber* core top measurements[7]. To represent both data sets in the same graph (Fig. 3) we converted the $\delta^{18}O_F$ core top measurements into seawater $\delta^{18}O_W$ values by using the temperature equation of Duplessy *et al.*[25] established for living *G. ruber* in the Indian Ocean.

The $\delta^{18}O$/salinity slope of 0.37 of the composite data set is probably the best value of c to be used in equations (4) and (5) to quantify the salinity variations at the location of Core MD900963. In order to illustrate the uncertainty associated with the conversion of $\delta^{18}O$ into surface salinity, we also used the individual slopes obtained for the two basins Arabian Sea and Bay of Bengal (dashed lines on Fig. 4*a* and 4*b*). Taking into account the standard reproducibility (±1 sigma) on the SST (±0.3 °C; ref. 17), on $\delta^{18}O_{WG}$ (±0.07‰; ref. 29) and on $\delta^{18}O_F$ (±0.05‰; ref. 30), it is possible to estimate an average analytical error of about ±0.3‰ for the reconstructed Δ salinity values. This indicates that only the major trends of the S and ΔS records should be interpreted in term of palaeoceanographic variations.

Figure 4*a* shows the downcore ΔS changes (equation (5)) whereas Fig. 4*b* presents the corresponding S values which take into account the global salinity variation due to sea level changes (equation 4). In the following paragraph we will mainly discuss the ΔS changes which are only due to local variations of the $E-P$ balance.

Negative ΔS values of about −1 to −0.5‰ are observed between 125 and 115 kyr BP (stage 5.5) and between 9 and 6 kyr

(Holocene). Between 160 and 140 kyr (stages 6.4 and 6.3) and between 75 and 25 kyr (stages 5.0 to 3.1), ΔS is consistently positive with values ranging between 0.5 to 1‰. Three short periods of elevated ΔS are clearly present in the record with values higher than 1‰: 140 to 125 kyr (stages 6.2 to 6.0), 90 to 80 kyr (stage 5.2) and 20 to 15 kyr (stage 2).

Negative ΔS during stage 5.5 and the early Holocene indicate that $E-P$ was lower than today. Because the precipitation over India and the Indian Ocean is related to the SW monsoon strength[3], the ΔS index suggests that the SW monsoon was stronger during these time intervals.

The higher ΔS values observed during glacial stages 6 and 2 and substage 5.2 on the Core site MD900963 were probably caused by increased evaporation and/or decreased precipitation. Consequently, it can be suggested that the dry NE monsoon was the dominating seasonal feature during these periods and/or that the humid SW monsoon was weakened. The generally high values obtained for the ΔS index (with the exception of stage 5.5 and the Holocene) suggest that in this part of the Indian Ocean the $E-P$ budget was different from the conditions of today during most of the last glacial cycle.

Based on pollen and foraminifera data[4-6], oxygen and carbon isotope composition of planktonic foraminifera[7,8] and organic matter content[8] similar climatic conditions were suggested for the LGM. During the LGM the decrease in precipitation led to considerably higher salinities in the Bay of Bengal due to the lower riverine freshwater input[5]. Our work extends these studies, and also shows that the Indian monsoon underwent large variations concomitant with the last global glacial-interglacial transition. Further SST determinations and salinity reconstructions are still necessary for the two basins (Arabian Sea and Bay of Bengal) both in order to calculate and model the changes of E and P independently and to understand in detail the climatology of the northern Indian Ocean during glacial periods. It will also be important to study the time variations of the marine productivity in the monsoonal upwelling zones off Somalia and Arabia, and their relationships with the salinity index reconstructed in this paper. □

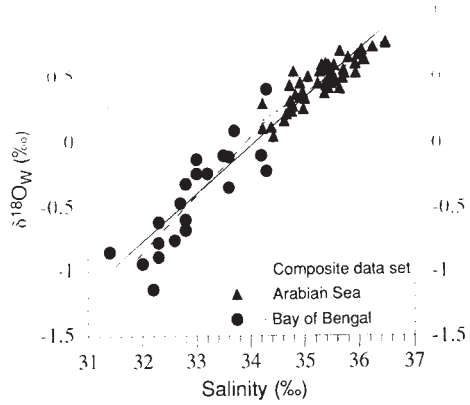

FIG. 3 $\delta^{18}O_W$/salinity relationships for the Arabian Sea and the Bay of Bengal. Regression lines were calculated for these two basins and for the composite data set as follows; Arabian Sea, $y=-9.24+0.28x$ ($R=0.87$); Bay of Bengal, $y=-15.20+0.45x$ ($R=0.87$); composite data set, $y=-12.68+0.37x$ ($R=0.95$). For this graph we used 52 seawater $\delta^{18}O_W$ and salinity measurements between 20° S and 21° N from the Arabian Sea (J. C. Duplessy, unpublished data). For the Bay of Bengal, a $\delta^{18}O_W$/salinity relationship was established by using 22 $\delta^{18}O_F$ G. *ruber* core top measurements[7]. To represent both data sets in the same graph the $\delta^{18}O_F$ core top measurements were converted into seawater $\delta^{18}O_W$ values by using the temperature equation of Duplessy *et al.*[25] established for living G. *ruber* in the Indian Ocean, and by taking into account a $\delta^{18}O$ enrichment of about 0.85‰ due to late calcification[25].

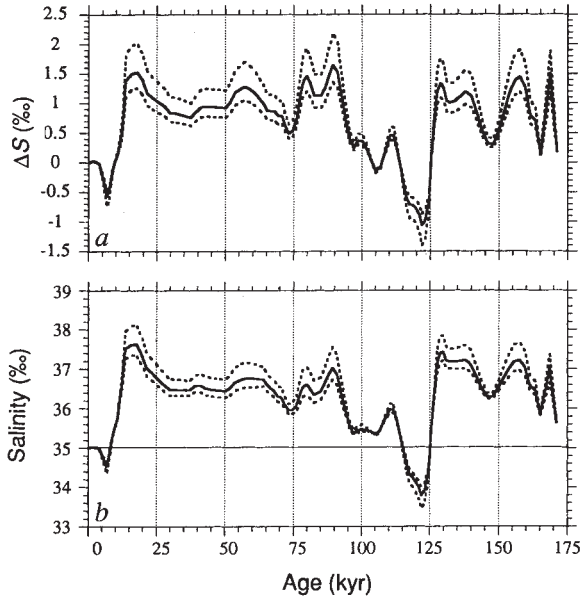

FIG. 4 *a*, Salinity variations ΔS for Core site MD900963. To eliminate high frequency variations due to the subtraction of two independent isotope records, we applied a least square filter to the salinity curves[31]. ΔS changes are calculated for the different slopes (C) of the $\delta^{18}O_W$ versus salinity relationships of the Arabian Sea (upper stippled line =0.28), the Bay of Bengal (lower stippled line =0.45) and the composite data set (solid line =0.37). ΔS values are directly related to local variations of the $E-P$ balance. *b*, Local salinity variations S for Core site MD900963, taking into account salinity changes due to changes of global ice volume. The modern salinity of Core site MD900963 is taken as 35‰ (ref. 21).

Received 28 January 1993; accepted 1 June 1993.

1. Brassell, S. C., Eglinton, G., Marlowe, I. T., Pflaumann, U. & Sarnthein, M. *Nature* **320,** 129–133 (1986).
2. Prahl, F. G. & Wakeham, S. G. *Nature* **330,** 367–369 (1987).
3. Cadet, D. & Reverdin, G. *Tellus* **33,** 476–487 (1981).
4. Van Campo, E. *Quat. Res.* **26,** 378–388 (1986).
5. Cullen, J. L. *Palaeogeogr. Palaeoclimatol. Palaeoecol.* **35,** 315 356 (1981).
6. Prell, W. A., *et al. Quat. Res.* **14,** 309–336 (1980).
7. Duplessy, J. C. *Nature* **295,** 494–497 (1982).
8. Fontugne, M. R. & Duplessy, J. C. *Palaeogeogr. Palaoclimatol. Palaeoecol.* **56,** 69 88 (1986).
9. Wyrtki, K. in *The Biology of the Indian Ocean* (ed. Zeitschel, B.) 18 36 (Springer, New York, 1973).
10. Bearman, G. (ed.) *Ocean Circulation* (Pergamon, Oxford, 1991).
11. Wyrtki, K. *Oceanographic Atlas of the International Indian Ocean Expedition* 531 (National Science Foundation, Washington DC 1971).
12. Bassinot, F. thesis, Univ. Aix-Marseille III (1993).
13. Imbrie, J. *et al.* in *Milankovitch and Climate. Part I* (eds Berger, A., Imbrie, J., Hays, J., Kukla, G. & Saltzman, B.), NATO ASI Series **126,** 269 305 (1984).
14. Prahl, F. G., Muehlhausen, L. A. & Lyle, M. *Geochim. cosmochim. Acta* **52,** 2303 2310 (1988).
15. Müller, P. J., Schneider, R. & Ruhland, G., in *Carbon Cycling in the Glacial Ocean: constraints on the Oceans Role in Global Climate Change* (eds Zahn, R., Kaminski, M. & Pedersen, T. F.) NATO ASI Series (in the press.)
16. Prell, W. A. & Hutson, W. A. *Science* **206,** 454 456 (1979).
17. Clemens, S., Prell, W. A., Murray, D., Shimmield, G. & Weedon, G. *Nature* **353,** 720 725 (1991).
18. Wüst, G., Brogmus, W. & Noodt, E. N. *Kieler Meeresforsch.* **10,** 137 161 (1954).
19. Craig, H. & Gordon, L. I. in *Spoleto Conference in Nuclear Geology* (ed. Tongiorgi E.) 9–130 (CNR, Pisa, 1965).
20. Broecker, W. S. *Paleoceanogr.* **4**(2), 207 212 (1989).
21. Levitus, S. in *NOAA Prof. Pap.* Vol. 13 (US Government Printing Office, Washington DC. 1982).
22. Nair, R. R. *et al. Nature* **338,** 749 751 (1989).
23. Curry, W. B., Ostermann, D. R., Guptha, M. V. S. & Ittekkot, V. in *Upwelling Systems: Evolution since the Early Miocene* (eds Summerhayes, C. P., Prell, W. L. & Emeis, K. C.) No. 64, 93 106 Geol. Soc. Spec. Publ. No. **64,** London, 1992.
24. Ittekkot, V., Haake, B., Bartsch, M., Nair, R. R. & Ramaswamy, V. in: *Upwelling Systems: Evolution since the Early Miocene.* (eds Summerhayes, C. P., Prell, W. L. & Emeis, K. C.) No. 64, 167 176 Geol. Soc. Spec. Publ. London, 1992.
25. Duplessy, J. C., Blanc, J. P. & Bé, A. W. H. *Science* **213,** 1247 1250 (1981).
26. Labeyrie L. D., Duplessy, J. C. & Blanc, P. L. *Nature* **327,** 477 482 (1987).
27. Vogelsang, E. thesis, Univ. Kiel (1990).
28. Fairbanks, R. G. *Nature* **342,** 637 642 (1989).
29. Labeyrie, L. D. & Duplessy, J. C. *Paleogeogr. Palaeoclimatol. Paleoecol.* **50,** 217 240 (1985).
30. Labeyrie, L. D. *et al. Quat. Sci. Rev.* **121,** 401 413 (1992).
31. Savitzky, A. & Golay, M. J. E. *Anal. Chem.* **36**(8), 1627 1639 (1964).

ACKNOWLEDGEMENTS. We thank E. Vincent, L. Beaufort, J. C. Duplessy, J. Volkman for discussions, J. C. Duplessy for providing unpublished $\delta^{18}O$ data, L. Beaufort for sharing unpublished informations on the coccoliths of core MD900963, B. LeCoat and J. Antignac for help in the isotopic analysis and N. Buchet for technical help with the samples. This research is supported by PNEDC, GDR PROMESSE and JE DRED 192.